International Journal of Medicine
pISSN 1468-3814 | eISSN 2667-7008
https://theinternationalmedicine.com/

Original Researcher Article *DOI: 10.61336/im/26-09-29*

Benign And Malignant Causes Of Palpable Breast Masses: Imaging Spectrum And Clinicopathological Correlation.

Dr. Rajkumari Rawat[1], Dr. Faraz Uddin Ansari[2]*, Dr. Fahad Uddin Ansari[3], Dr. Yash Yadav[4].

[1]Assistant Professor, Department of Radio-diagnosis., Sri Aurobindo Medical College & P.G. Institute, Indore.

[2]PG Resident, Department of Radio-diagnosis, Sri Aurobindo Medical College & P.G. Institute, Indore.

[3]Senior Resident, Department of Plastic surgery, Aligarh Muslim University, Aligharh

[4]PG Resident, Department of Radio-diagnosis, Sri Aurobindo Medical College & P.G. Institute, Indore.

Correspondence:
Dr. Faraz Uddin Ansari.
PG Resident, Department of Radio-diagnosis, Sri Aurobindo Medical College & P.G. Institute, Indore.

Received: 03-08-2026
Revised: 14-08-2026
Accepted: 29-08-2026
Published: 04-09-2026

Abstract

Background: Palpable breast masses require timely evaluation because clinical examination alone cannot reliably distinguish benign from malignant lesions. Ultrasonography provides detailed structural characterization, while 18F-FDG PET/CT offers complementary metabolic and staging information. This study evaluated the diagnostic performance of both modalities against histopathology. ***Methods:*** This prospective cross-sectional observational study included 45 patients with palpable breast masses who underwent breast ultrasonography and ^18F-FDG PET/CT followed by histopathological evaluation. Sonographic characteristics including echogenicity, margins, shape, vascularity, and BI-RADS category were assessed. PET/CT findings included lesion morphology, FDG uptake, SUVmax, and axillary nodal involvement. Diagnostic performance and agreement with histopathology were analyzed. ***Results:*** The mean age was 51.20 ± 13.52 years, with 53.3% of patients aged 40–59 years. Histopathology demonstrated 32 (71.1%) malignant and 13 (28.9%) benign lesions, with invasive ductal carcinoma being the most common diagnosis (42.2%). Hypoechogenicity, irregular margins, lobulated/irregular morphology, vascularity, and higher BI-RADS categories were significantly associated with malignancy ($p<0.05$). Sonography demonstrated 93.8% sensitivity, 92.3% specificity, 96.8% positive predictive value, 85.7% negative predictive value, and 93.3% diagnostic accuracy, with excellent agreement with histopathology ($\kappa=0.86$). PET/CT showed 90.6% sensitivity, 92.3% specificity, 96.7% positive predictive value, 80.0% negative predictive value, and 91.1% diagnostic accuracy ($\kappa=0.82$). SUVmax showed excellent discriminatory ability for malignancy (AUC=0.929). ***Conclusion:*** Sonography demonstrated slightly superior diagnostic performance for local characterization of palpable breast masses, whereas PET/CT provided valuable complementary metabolic and staging information. Their combined interpretation may enhance diagnostic confidence, while histopathology remains essential for definitive diagnosis.

Keywords: Palpable breast mass; Ultrasonography; 18F-FDG PET/CT; SUVmax; Histopathology.

INTRODUCTION

Palpable breast masses are common clinical presentations requiring diagnostic imaging. Although many are benign, the possibility of malignancy necessitates accurate and timely evaluation. Clinical examination confirms the presence of a mass but may not reliably determine its pathological nature, particularly in dense breasts or inflammatory conditions. Thus, imaging plays a pivotal role in characterizing lesion morphology, extent, regional nodal involvement, and, when required, systemic disease [1].

Ultrasonography is a widely used, non-invasive, non-ionizing modality for evaluating palpable breast masses. It is particularly useful in younger women and patients with dense breasts and permits differentiation of cystic and solid lesions while assessing margins, echotexture, orientation, and posterior acoustic features. Standardized interpretation using the BI-RADS lexicon facilitates risk stratification and management [2,3]. However, overlap between benign and malignant appearances and operator dependence may cause diagnostic uncertainty.

18F-FDG positron emission tomography/computed tomography (PET/CT) provides functional and metabolic information complementary to anatomical imaging. Increased FDG uptake is frequently associated with malignancy, while PET/CT also permits assessment of regional and distant disease, contributing to staging, treatment planning, response assessment,

and detection of recurrence [5,6]. Whole-body imaging may be particularly useful in patients with clinically suspicious or advanced lesions [7,8].

However, FDG uptake is not specific for malignancy, as inflammatory, infectious, granulomatous, and some benign lesions may demonstrate increased uptake, whereas certain low-grade malignancies may show relatively low activity [9,10]. PET/CT should therefore be interpreted alongside anatomical imaging and clinical findings. Ultrasound and PET/CT provide complementary structural and functional information, respectively [11], while histopathology remains the reference standard for definitive diagnosis and imaging correlation [12,13].The present study aimed to assess the utility of PET/CT and sonography in evaluating palpable breast masses, characterize their imaging spectrum, correlate imaging findings with histopathology, and highlight common and uncommon causes of these lesions.

MATERIALS AND METHODS

This hospital-based prospective cross-sectional analytical observational study was conducted in the Department of Radiodiagnosis, Sri Aurobindo Medical College and Post Graduate Institute (SAMC & PGI), Indore, Madhya Pradesh, India, over a period of 18 months from June 2024 to November 2025, following approval from the Institutional Ethics Committee.

Written informed consent was obtained from all participants before enrollment. Patient confidentiality was maintained throughout the study, and participation was voluntary without affecting routine clinical management. Breast ultrasonography and 18F-FDG PET/CT were performed as part of the clinical evaluation, and no additional intervention was undertaken solely for study participation.

Inclusion and Exclusion Criteria

Patients of all age groups and either sex presenting with a clinically palpable breast mass and undergoing both breast ultrasonography and 18F-FDG PET/CT during the study period were eligible for inclusion. Patients who declined written informed consent and those with an absolute contraindication to PET imaging were excluded. A total of 35 eligible patients were enrolled using consecutive sampling during the study period.

Methodology

Patients with palpable breast masses were identified and approached for participation after obtaining informed consent. Baseline information including demographic characteristics, clinical history, presenting complaints, duration of the breast lump, associated pain or nipple discharge when present, clinical examination findings, and provisional clinical diagnosis were recorded using a predesigned structured proforma before imaging. Consecutive sampling was used, and all eligible patients presenting during the study period were considered for enrollment.

Ultrasonographic Examination and Image Analysis

Breast ultrasonography was performed as part of the routine diagnostic evaluation, with assessment of the breast lesion and regional axillary lymph nodes. The lesion was evaluated for laterality and anatomical location, size, shape, margins, orientation, echogenicity, internal composition, and posterior acoustic characteristics. Associated findings, including skin thickening, ductal dilatation, and edema, were documented. Axillary lymph nodes were assessed for suspicious morphological features, including cortical thickening and loss of the fatty hilum. The final sonographic impression was recorded for each lesion.

18F-FDG PET/CT Examination and Image Analysis

18F-FDG PET/CT was subsequently performed according to the institutional nuclear medicine protocol. The breast lesion was assessed for the presence and pattern of FDG uptake, with documentation of metabolic activity and SUV-based assessment where available. Regional lymph nodes, including axillary, internal mammary, and supraclavicular stations, were evaluated for abnormal metabolic activity. Whole-body PET/CT images were reviewed for evidence of distant metastatic disease involving the lungs, liver, bones, distant lymph nodes, or other organs. The final PET/CT impression was documented for each participant.

Histopathological Correlation

Where clinically indicated, biopsy or surgical excision was performed following imaging evaluation. Histopathological diagnosis obtained from biopsy or surgical specimens was considered the reference standard for clinicopathological correlation. Lesions were classified as benign or malignant according to the final pathological diagnosis, and the imaging findings on ultrasonography and PET/CT were compared with the corresponding histopathological findings.

Study Procedure and Data Collection

Clinical, sonographic, PET/CT, histopathological, and final diagnostic findings were recorded in a standardized proforma and master chart. The study did not alter the routine clinical management of the participants.

Outcome Measures

The primary outcomes were the imaging characteristics of palpable breast masses on ultrasonography and 18F-FDG PET/CT and their correlation with the final histopathological diagnosis. Secondary outcomes included the demographic and clinical profile of the participants, frequency and distribution of benign and malignant lesions, sonographic characteristics, PET/CT metabolic characteristics, regional nodal involvement, distant metastatic disease, and areas of concordance or discordance between the two imaging modalities and histopathology.

Statistical Analysis

Data were analyzed using R statistical software. Continuous variables were expressed as mean ± standard deviation and categorical variables as frequencies and percentages. Associations were assessed using the Chi-square or Fisher's exact test, as appropriate. Sensitivity, specificity, and concordance with histopathology were calculated for ultrasonography and 18F-FDG PET/CT. A p-value <0.05 was considered statistically significant.

RESULTS

Demographic, Clinical, and Tumor Characteristics: A total of 45 patients with palpable breast masses were evaluated. The mean age was 51.20 ± 13.52 years (range, 25–72 years), with the 40–59-year age group representing the largest proportion (53.3%). The right breast was involved in 53.3% of cases. Most lesions were non-tender (84.4%) and immobile (62.2%), while local warmth was absent in 82.2%. Clinically palpable axillary lymph nodes were present in 51.1% of patients. The upper outer quadrant was the most frequently involved site (51.1%), and skin changes were present in 28.9% of cases. The mean tumor size was 3.18 ± 1.48 cm (range, 0.8–7.4 cm), and the mean SUVmax was 6.76 ± 4.47 (range, 1.1–18.4). [Table 1]

Table 1. Demographic, Clinical, and Tumor Characteristics of Study Participants (n=45)

Variable	Category	n (%)
Age group	25–39 years	11 (24.4)
	40–59 years	24 (53.3)
	≥60 years	10 (22.2)
Side	Right	24 (53.3)
	Left	21 (46.7)
Tenderness	Tender	7 (15.6)
	Non-tender	38 (84.4)
Mobility	Mobile	17 (37.8)
	Immobile	28 (62.2)
Warmth	Present	8 (17.8)
	Absent	37 (82.2)
Clinical axillary nodes	Present	23 (51.1)
	Absent	22 (48.9)
Location	Upper outer quadrant	23 (51.1)
	Other quadrants	22 (48.9)
Skin changes	Present	13 (28.9)
	Absent	32 (71.1)

Ultrasonographic and PET/CT Characteristics: On ultrasonography, hypoechoic lesions predominated (91.1%). Irregular margins were more frequent than regular margins (64.4% vs. 35.6%), and lobulated/irregular morphology was the most frequent sonographic shape (53.3%). Increased vascularity was present in 46.7% of lesions. BI-RADS 5 was the most frequent category (44.4%), while BI-RADS 2 and 3 accounted for 13.3% and 11.1%, respectively. The reported sonographic impression classified 32 lesions as malignant and 13 as benign.

On PET/CT, irregular margins were observed in 64.4% of lesions. Round, oval, and lobulated morphologies accounted for 35.6%, 33.3%, and 31.1%, respectively. High FDG uptake (SUVmax ≥2.5) was observed in 86.7% of lesions. PET/CT classified 30 lesions (66.7%) as malignant and 15 (33.3%) as benign. Axillary nodes were present on PET/CT in 48.9% of cases. On ultrasonography, axillary nodes were present in 51.1% of cases, with necrotic morphology in 55.6% and maintained hilar architecture in 44.4%. [Table 2]

Table 2. Imaging Characteristics of Palpable Breast Lesions

Modality/Parameter	Category	n (%)
USG Characteristics		
USG echogenicity	Anechoic	2 (4.4)
	Hyperechoic	2 (4.4)
	Hypoechoic	41 (91.1)
USG margin	Regular	16 (35.6)
	Irregular	29 (64.4)
USG shape	Round	10 (22.2)
	Oval	11 (24.4)
	Lobulated/irregular	24 (53.3)
USG vascularity	Absent	24 (53.3)
	Present	21 (46.7)
USG BI-RADS	2	6 (13.3)
	3	5 (11.1)
	4A	4 (8.9)
	4B	5 (11.1)
	4C	5 (11.1)
	5	20 (44.4)
USG diagnosis	Benign	13 (28.9)
	Malignant	32 (71.1)
PET Characteristics		
PET margin	Smooth	16 (35.6)
	Irregular	29 (64.4)
PET shape	Round	16 (35.6)
	Oval	15 (33.3)
	Lobulated	14 (31.1)
SUVmax group	<2.5	6 (13.3)
	≥2.5	39 (86.7)
PET diagnosis	Benign	15 (33.3)
	Malignant	30 (66.7)
Axillary nodes on PET	Absent	23 (51.1)
	Present	22 (48.9)
Axillary nodes on USG	Absent	22 (48.9)
	Present	23 (51.1)
USG nodal morphology	Maintained hilum	20 (44.4)
	Necrotic	25 (55.6)

The association between axillary nodal status and PET SUVmax was statistically significant (p=0.009). Among lesions without axillary nodal involvement, 72.7% demonstrated high SUVmax, whereas all lesions with axillary nodal involvement demonstrated high SUVmax.

Histopathological Spectrum: Histopathological examination demonstrated 32 malignant lesions (71.1%) and 13 benign lesions (28.9%). Invasive ductal carcinoma was the most common diagnosis (42.2%), followed by fibroadenoma (11.1%) and invasive lobular carcinoma (8.9%). The remaining lesions comprised a spectrum of benign, malignant, and less common breast pathologies. [Table 3]

Table 3. Histopathological Spectrum of Palpable Breast Lesions

Histopathological diagnosis	n (%)
Invasive ductal carcinoma	19 (42.2)
Fibroadenoma	5 (11.1)
Invasive lobular carcinoma	4 (8.9)
Fibrocystic disease	3 (6.7)
Ductal carcinoma in situ	2 (4.4)
Breast abscess	2 (4.4)
Mucinous carcinoma	2 (4.4)
Medullary carcinoma	2 (4.4)

Triple-negative/inflammatory breast carcinoma	2 (4.4)
Fat necrosis	1 (2.2)
Lipoma	1 (2.2)
Benign phyllodes tumor	1 (2.2)
Malignant phyllodes tumor	1 (2.2)
Encapsulated papillary carcinoma	1 (2.2)
Total	45 (100)

Correlation of Sonographic Findings With Histopathology: Sonographic echogenicity was significantly associated with final histopathological diagnosis (p=0.005). Hypoechoic lesions constituted all malignant lesions in the reported cross-tabulation. Margin characteristics were also significantly associated with malignancy (p=0.003), with irregular margins observed in 81.3% of malignant lesions compared with 23.1% of benign lesions. Lesion shape showed a significant association with histopathology (p<0.01), with lobulated/irregular lesions predominantly malignant.

Vascularity demonstrated a strong association with malignancy (p<0.001); all lesions showing vascularity were malignant in the reported cross-tabulation. BI-RADS category was significantly associated with histopathological diagnosis (p<0.001). All BI-RADS 2 and 3 lesions were benign, BI-RADS 4A lesions showed an equal distribution of benign and malignant pathology, and all BI-RADS 4B, 4C, and 5 lesions were malignant. The reported sonographic diagnostic impression also showed excellent agreement with histopathology (κ=0.86, p<0.001). [Table 4]

Table 4. Association of Sonographic Characteristics and BI-RADS With Histopathological Diagnosis

USG parameter	Category	Benign n (%)	Malignant n (%)	p-value
Echogenicity	Anechoic	2 (15.4)	0 (0.0)	0.005
	Hyperechoic	2 (15.4)	0 (0.0)	
	Hypoechoic	9 (69.2)	32 (100.0)	
Margin	Regular	10 (76.9)	6 (18.8)	0.003
	Irregular	3 (23.1)	26 (81.3)	
Shape	Round	3 (23.1)	0 (0.0)	<0.01
	Oval	9 (69.2)	4 (12.5)	
	Lobulated/irregular	1 (7.7)	28 (87.5)	
Vascularity	Absent	13 (100.0)	11 (34.4)	<0.001
	Present	0 (0.0)	21 (65.6)	
BI-RADS	2	6 (100.0)	0 (0.0)	<0.001
	3	5 (100.0)	0 (0.0)	
	4A	2 (50.0)	2 (50.0)	
	4B	0 (0.0)	5 (100.0)	
	4C	0 (0.0)	5 (100.0)	
	5	0 (0.0)	20 (100.0)	

Correlation of PET/CT Findings With Histopathology: PET margin characteristics were significantly associated with final diagnosis. Smooth margins were observed in 69.2% of benign lesions and 21.9% of malignant lesions, whereas irregular margins were observed in 30.8% of benign and 78.1% of malignant lesions. PET lesion shape was not significantly associated with histopathological diagnosis (p=0.497). SUVmax demonstrated a strong association with malignancy (p<0.001): all six lesions with SUVmax <2.5 were benign, whereas 32 of 39 lesions with SUVmax ≥2.5 were malignant. PET diagnostic classification showed excellent agreement with histopathology (κ=0.82, p<0.001). [Table 5]

Table 5. Association of PET/CT Characteristics With Histopathological Diagnosis

PET parameter	Category	Benign n (%)	Malignant n (%)	p-value
Margin	Smooth	9 (69.2)	7 (21.9)	<0.001*
	Irregular	4 (30.8)	25 (78.1)	
Shape	Lobulated	3 (23.1)	11 (34.4)	0.497
	Oval	6 (46.2)	9 (28.1)	
	Round	4 (30.8)	12 (37.5)	
SUVmax	<2.5	6 (46.2)	0 (0.0)	<0.001
	≥2.5	7 (53.8)	32 (100.0)	

Concordance Between Sonography and PET/CT: A significant association was observed between sonographic vascularity and PET SUVmax category (p=0.014). All six lesions with low SUVmax showed absent vascularity, whereas

all 21 vascular lesions demonstrated high SUVmax. Sonographic vascularity had a sensitivity of 53.8%, specificity of 100%, positive predictive value of 100%, negative predictive value of 25%, and accuracy of 60% for predicting high PET metabolic activity. ROC analysis yielded an AUC of 0.769, while the reported kappa was 0.269 (p=0.014), indicating fair agreement. Axillary nodal status was also significantly associated with PET SUVmax category (p=0.009); all lesions with axillary nodes demonstrated high SUVmax, compared with 72.7% of lesions without nodal involvement.

Sonographic margin characteristics showed strong concordance with PET margin characteristics. The sensitivity, specificity, PPV, NPV, and accuracy of sonographic margins for predicting PET margin characteristics were 100%, 78.6%, 90.3%, 100%, and 92.9%, respectively. The AUC was 0.893 and kappa was 0.850 (p<0.001), indicating excellent agreement. No statistically significant association was observed between sonographic and PET lesion shape (χ^2=13.157, df=10, p=0.215). The combined correlation analysis further demonstrated significant associations between BI-RADS category and final diagnosis (p<0.001), sonographic shape and final diagnosis (p=0.003), PET margin characteristics and final diagnosis (p=0.005), and SUVmax group and final diagnosis (p<0.001).

Table 6. Concordance and Intermodality Associations Between Sonography and PET/CT

Analysis	Parameter	Result
USG vascularity vs. PET SUVmax	Sensitivity	53.8%
	Specificity	100.0%
	PPV	100.0%
	NPV	25.0%
	Accuracy	60.0%
	AUC	0.769
	Kappa	0.269 (p=0.014)
USG margin vs. PET margin	Sensitivity	100.0%
	Specificity	78.6%
	PPV	90.3%
	NPV	100.0%
	Accuracy	92.9%
	AUC	0.893
	Kappa	0.850 (p<0.001)
USG shape vs. PET shape	χ^2	13.157
	df	10
	p-value	0.215
Axillary nodal status vs. PET SUVmax	p-value	0.009
BI-RADS vs. final diagnosis	p-value	<0.001
USG shape vs. final diagnosis	p-value	0.003
PET margin vs. final diagnosis	p-value	0.005
SUVmax group vs. final diagnosis	p-value	<0.001

ROC analysis demonstrated excellent discriminatory performance of SUVmax for differentiating benign from malignant lesions, with an AUC of 0.929. Overall, sonography demonstrated slightly higher sensitivity and diagnostic accuracy than PET/CT, while both modalities showed the same reported specificity of 92.3%.

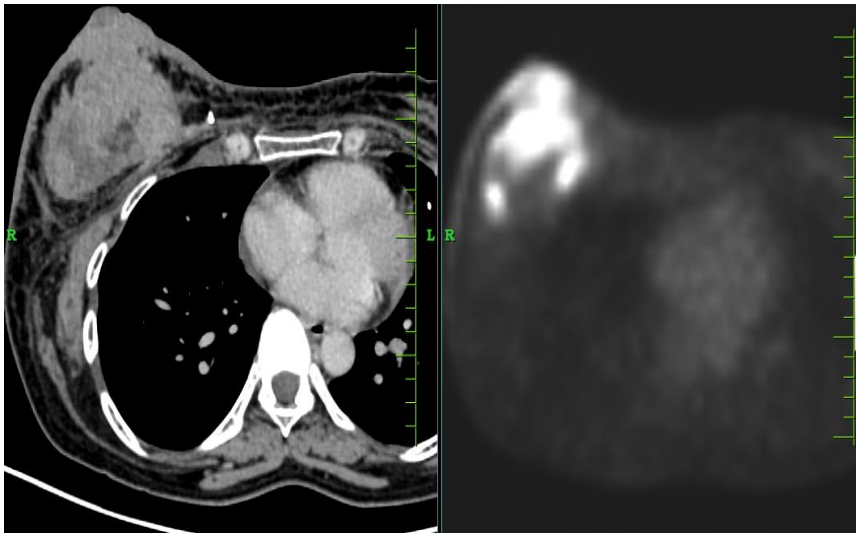

Figure 1: 18F-FDG PET/CT demonstrating a metabolically active right breast mass. Increased FDG uptake is seen within a large, heterogeneously enhancing soft-tissue-density mass in the right breast involving the nipple–areolar complex, measuring approximately 8.9 × 5.2 × 8.5 cm, with a SUVmax of 19.7. Posteriorly, the lesion closely abuts the pectoralis major muscle with loss of the intervening fat plane. The marked metabolic activity, large size, heterogeneous enhancement, and local involvement are consistent with the known malignant breast pathology.

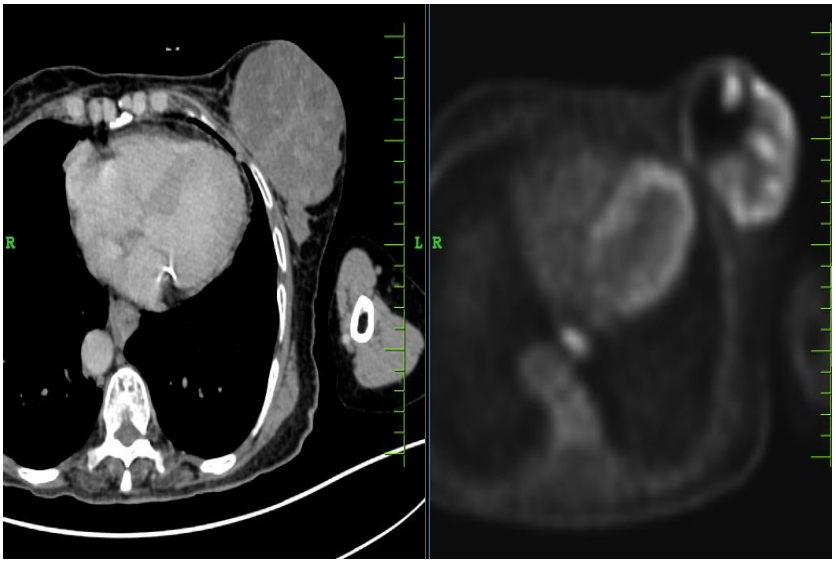

Figure 2. 18F-FDG PET/CT demonstrating a metabolically active left breast mass Increased FDG uptake is noted within a heterogeneously enhancing, partly necrotic soft-tissue-density mass involving almost the entire left breast, measuring approximately 8.5 × 6.0 cm, with a SUVmax of 8.4. The lesion infiltrates the overlying skin and abuts the underlying muscle, with preservation of the intervening fat planes. The presence of marked metabolic activity, heterogeneous enhancement, necrotic areas, and skin infiltration is consistent with the known malignant breast pathology.

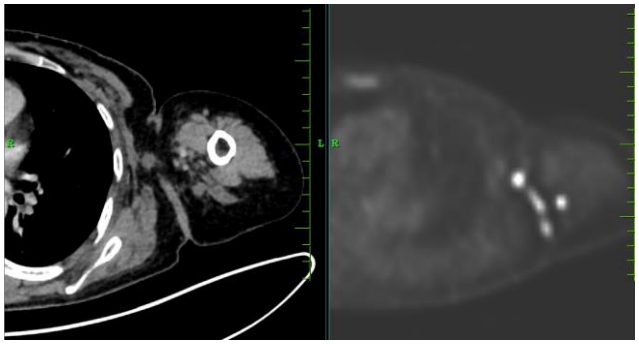

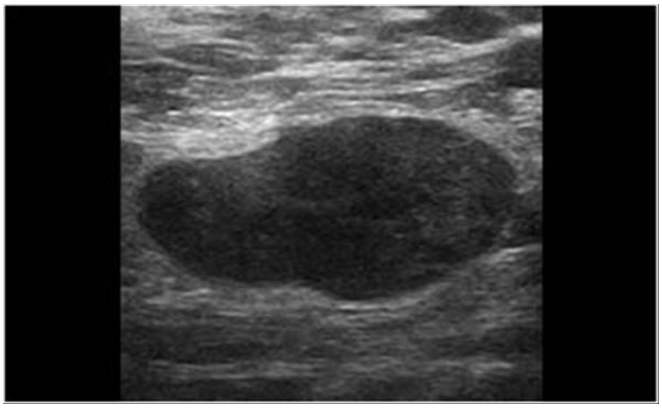

Figure 3. 18F-FDG PET/CT and ultrasonographic demonstration of metastatic axillary lymphadenopathy Multiple FDG-avid bilateral axillary and deep pectoral lymph nodes are noted, with the largest measuring approximately 1.5 × 1.1 cm and demonstrating a SUVmax of 9.5. Ultrasonography demonstrates an enlarged necrotic lymph node in the left axilla. The combined metabolic and morphological findings are suggestive of metastatic axillary lymph-node involvement in a known case of left breast carcinoma.

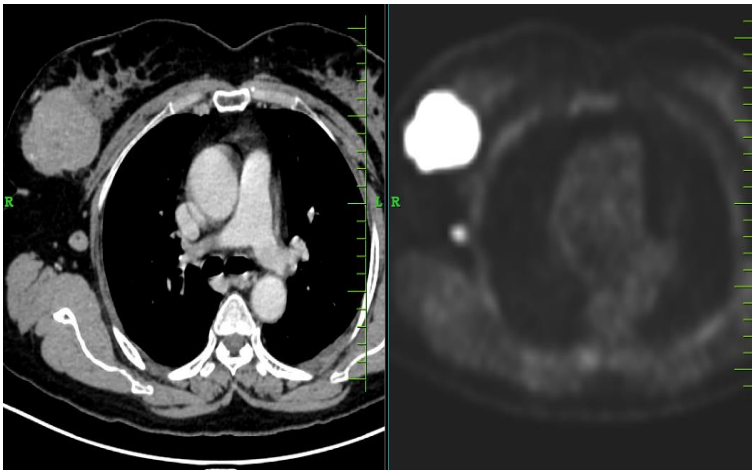

Figure 4. 18F-FDG PET/CT demonstrating a metabolically active right breast mass. Increased FDG uptake is noted within a large, heterogeneously enhancing, irregular soft-tissue-density mass in the upper outer quadrant of the right breast, measuring approximately 5.6 × 5.2 cm, with a SUVmax of 24.3. The marked metabolic activity and irregular morphology are highly suspicious for malignancy and are consistent with the known malignant breast pathology.

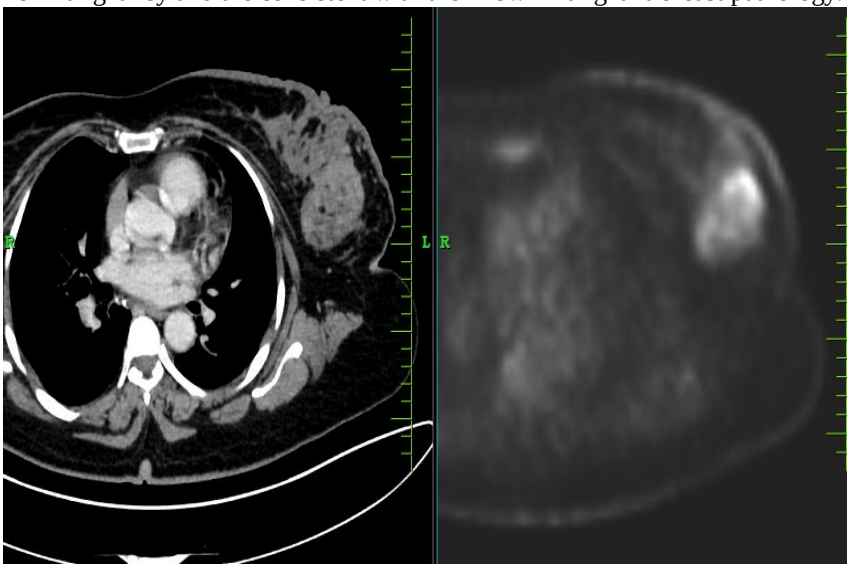

Figure 5. 18F-FDG PET/CT demonstrating metabolically active left breast lesions. Increased FDG uptake is noted within heterogeneously enhancing soft-tissue-density lesions involving the upper outer and lower outer quadrants of the left breast. The largest lesion measures approximately 2.1 × 1.2 cm, with a SUVmax of 20.6. The presence of metabolically active

breast nodules with markedly increased FDG uptake is suspicious for malignant pathology and should be correlated with the corresponding sonographic and histopathological findings.

DISCUSSION

The present study evaluated the sonographic and ^18F-FDG PET/CT characteristics of 45 patients with palpable breast masses and correlated the imaging findings with histopathology. Malignant lesions predominated, accounting for 32 (71.1%) cases, while 13 (28.9%) were benign. Invasive ductal carcinoma was the most common diagnosis (19, 42.2%), followed by fibroadenoma (5, 11.1%) and invasive lobular carcinoma (4, 8.9%). The relatively high malignant proportion may reflect the tertiary-care setting and selection of patients undergoing PET/CT, which is generally performed in clinically or radiologically suspicious cases. Panareo et al. reported a comparable malignancy rate of 68.2% among lesions demonstrating focal morphologic and metabolic abnormalities [14]. In contrast, Job et al. and Runjjala and Naidu reported malignancy rates of 45.3% and 34.62%, respectively [15,16]. These differences likely reflect variations in referral patterns, patient selection, and the use of advanced metabolic imaging.

The mean age was 51.20 ± 13.52 years, with the 40–59-year group comprising the largest proportion (53.3%). This middle-aged predominance is clinically relevant given the increasing risk of breast malignancy with age. Similar adult populations with palpable breast abnormalities were evaluated by Runjjala and Naidu and Kanumuri et al., who emphasized the importance of timely imaging assessment [16,17]. Right-sided lesions were slightly more frequent than left-sided lesions (53.3% vs. 46.7%), although this difference has limited diagnostic significance. Most lesions were non-tender (84.4%), lacked warmth (82.2%), and were immobile (62.2%). While this clinical pattern is more suggestive of neoplastic rather than acute inflammatory pathology, benign lesions may mimic malignancy. Moschetta et al. demonstrated that diabetic mastopathy can present as an irregular hypoechoic mass despite being benign [18]. Thus, clinical findings should guide suspicion but cannot substitute for imaging and pathological confirmation.

Axillary lymph nodes were clinically identified in 51.1% of patients, and the upper outer quadrant was the most frequent site of involvement (51.1%). The relatively high frequency of axillary involvement is clinically important because nodal status influences staging and treatment planning. Sohn et al. demonstrated the complementary value of PET/CT and sonography in axillary assessment, particularly when combined with image-guided FNA [19]. Skin changes were present in 28.9% of patients, indicating locally advanced or aggressive clinical features in a subset of cases.

On sonography, hypoechoic lesions predominated (91.1%), while irregular margins, lobulated or irregular morphology, and vascularity were observed in 64.4%, 53.3%, and 46.7% of lesions, respectively. BI-RADS 5 was the most frequent category (44.4%), consistent with the high-risk nature of the cohort. Hypoechogenicity, irregular margins, lesion shape, and vascularity showed significant associations with histopathology. In particular, irregular margins were significantly more frequent in malignant lesions, while all vascular lesions in the reported cohort were malignant. These findings support the established importance of combined sonographic morphological assessment. However, individual features lack absolute specificity. Moschetta et al. reported suspicious hypoechoic morphology in benign diabetic mastopathy, while Parashar et al. cautioned against relying on echogenicity alone for malignancy assessment [18,20]. Therefore, lesion morphology should be interpreted collectively using BI-RADS criteria.

BI-RADS category demonstrated a strong association with histopathology. All BI-RADS 2 and 3 lesions were benign, whereas BI-RADS 4B, 4C, and 5 lesions were malignant; BI-RADS 4A lesions showed equal benign and malignant distribution. Yücesoy et al. reported a 99.1% negative predictive value for BI-RADS 3 lesions, with only two malignancies among 213 cases [22]. The present finding of all five BI-RADS 3 lesions being benign supports the reliability of standardized BI-RADS-based risk stratification when appropriately applied.

PET/CT provided complementary metabolic information. Irregular PET margins were present in 64.4% of lesions, while high FDG uptake (SUVmax ≥2.5) was observed in 86.7%. PET margin characteristics were significantly associated with histopathology, whereas PET lesion shape was not. SUVmax demonstrated a particularly strong association with malignancy ($p<0.001$), and ROC analysis showed excellent discriminatory ability with an AUC of 0.929. However, high SUVmax was also present in 7 of 13 benign lesions, emphasizing that FDG uptake is not specific for malignancy. Fujioka et al. reported FDG uptake in 53.8% of DCIS lesions and noted greater uptake in larger or symptomatic lesions [23]. Conversely, Panareo et al. found no significant association between SUVmax alone and histopathology [14]. The higher metabolic activity in the present cohort may therefore reflect the predominance of palpable, relatively large, and invasive lesions.

The intermodality analysis demonstrated that sonography and PET/CT provide complementary rather than interchangeable information. Sonographic vascularity was significantly associated with high PET SUVmax ($p=0.014$), but agreement was only fair ($\kappa=0.269$). Vascularity showed 100% specificity and PPV but only 53.8% sensitivity for predicting high metabolic

activity, indicating that its presence strongly supported metabolic activity, whereas its absence could not exclude it. In contrast, sonographic and PET margin characteristics demonstrated excellent concordance, with 92.9% diagnostic accuracy, an AUC of 0.893, and κ=0.850. This suggests that structural margin assessment is more consistently reproduced between modalities than vascular and metabolic characteristics. Similarly, the lack of significant association between sonographic and PET lesion shape (p=0.215) indicates that PET morphology should not replace detailed sonographic structural assessment.

Axillary evaluation further demonstrated the complementary role of both modalities. PET/CT showed axillary nodal involvement in 48.9% of cases, compared with 51.1% on sonography. Importantly, axillary nodal involvement was significantly associated with high SUVmax (p=0.009), with all nodal-positive cases demonstrating high metabolic activity. These findings are consistent with Sohn et al., who demonstrated improved axillary assessment when PET/CT was combined with sonography [19]. Nevertheless, imaging-based nodal assessment should not replace tissue sampling when pathological confirmation is clinically required.

Overall, sonography demonstrated slightly better diagnostic performance than PET/CT. Sonography showed 93.8% sensitivity, 92.3% specificity, 96.8% PPV, 85.7% NPV, and 93.3% accuracy, compared with 90.6%, 92.3%, 96.7%, 80.0%, and 91.1%, respectively, for PET/CT. Agreement with histopathology was excellent for both modalities, with κ=0.86 for sonography and κ=0.82 for PET/CT. These findings are broadly consistent with previous studies reporting high diagnostic performance of sonography and combined breast imaging [15-18]. Kanumuri et al. reported 95.7% sensitivity and 100% PPV, whereas Runjjala and Naidu reported comparatively lower diagnostic performance [16,17]. The present results therefore support sonography as the principal modality for local characterization of palpable breast masses, with PET/CT serving as a valuable adjunct for metabolic characterization, nodal assessment, and whole-body staging. Histopathology remains essential in suspicious, indeterminate, or discordant lesions.

Limitations: The study was limited by its small sample size and single-center design, which may restrict generalizability. Selection bias was possible because patients undergoing PET/CT were likely to have clinically or radiologically suspicious lesions. The study lacked long-term follow-up, and histopathological correlation was available only when clinically indicated. Larger multicenter studies are warranted for validation.

CONCLUSION

Sonography and 18F-FDG PET/CT demonstrated high diagnostic performance in the evaluation of palpable breast masses, with excellent agreement with histopathology. Sonography showed slightly superior sensitivity and accuracy for benign-malignant differentiation, while PET/CT provided valuable metabolic and staging information. SUVmax demonstrated excellent discriminatory ability for malignancy (AUC 0.929). These findings support sonography as the primary modality for local lesion characterization, with PET/CT serving as a complementary tool in clinically or radiologically suspicious cases. Nevertheless, imaging cannot replace histopathological confirmation, particularly in lesions with atypical or discordant imaging features.

REFERENCES

1. Vadakekut ES, Puckett Y. New palpable breast mass. In: StatPearls [Internet]. Treasure Island (FL): StatPearls Publishing; 2025.
2. Expert Panel on Breast Imaging; Klein KA, Kocher M, Lourenco AP, Niell BL, Bennett DL, Chetlen A, et al. ACR Appropriateness Criteria® palpable breast masses: 2022 update. J Am Coll Radiol. 2023;20(5S):S146-S163. doi:10.1016/j.jacr.2023.02.013.
3. Raza S, Goldkamp AL, Chikarmane SA, Birdwell RL. US of breast masses categorized as BI-RADS 3, 4, and 5: pictorial review of factors influencing clinical management. Radiographics. 2010;30(5):1199-1213. doi:10.1148/rg.305095144.
4. Lehman CD, Lee AY, Lee CI. Imaging management of palpable breast abnormalities. AJR Am J Roentgenol. 2014;203(5):1142-1153. doi:10.2214/AJR.14.12725.
5. Hadebe B, Harry L, Ebrahim T, Pillay V, Vorster M. The role of PET/CT in breast cancer. Diagnostics (Basel). 2023;13(4):597. doi:10.3390/diagnostics13040597.
6. Groheux D, Cochet A, Humbert O, Alberini JL, Hindié E, Mankoff D. ^18F-FDG PET/CT for staging and restaging of breast cancer. J Nucl Med. 2016;57(Suppl 1):17S-26S. doi:10.2967/jnumed.115.157859.
7. Gunes A, Colapkulu-Akgul N, Akgul C, Unlu I, Cinar S. Axillary staging with ^18F-FDG PET/CT in early breast cancer: impact of tumor subtypes. Ann Saudi Med. 2025;45(3):145-153. doi:10.5144/0256-4947.2025.145.
8. Davidson T, Shehade N, Nissan E, Sklair-Levy M, Ben-Haim S, Barshack I, et al. PET/CT in breast cancer staging is useful for evaluation of axillary lymph node and distant metastases. Surg Oncol. 2021;38:101567. doi:10.1016/j.suronc.2021.101567

9. Adejolu M, Huo L, Rohren E, Santiago L, Yang WT. False-positive lesions mimicking breast cancer on FDG PET and PET/CT. AJR Am J Roentgenol. 2012 Mar;198(3):W304-14. doi: 10.2214/AJR.11.7130.
10. Lim HS, Yoon W, Chung TW, Kim JK, Park JG, Kang HK, Bom HS, Yoon JH. FDG PET/CT for the detection and evaluation of breast diseases: usefulness and limitations. Radiographics. 2007 Oct;27 Suppl 1:S197-213. doi: 10.1148/rg.27si075507.
11. Assi HI, Alameh IA, Khoury J, Bou Zerdan M, Akiki V, Charafeddine M, El Saheb GI, Sukhon F, Sbaity E, Baydoun S, Shabb N, Berjawi G, Haidar MB. Diagnostic Performance of FDG-PET/CT Scan as Compared to US-Guided FNA in Prediction of Axillary Lymph Node Involvement in Breast Cancer Patients. Front Oncol. 2021 Oct 1;11:740336. doi: 10.3389/fonc.2021.740336.
12. Shin KM, Kim HJ, Jung SJ, Lim HS, Lee SW, Cho SH, Jang YJ, Lee HJ, Kim GC, Jung JH, Park JY. Incidental Breast Lesions Identified by (18)F-FDG PET/CT: Which Clinical Variables Differentiate between Benign and Malignant Breast Lesions? J Breast Cancer. 2015 Mar;18(1):73-9. doi: 10.4048/jbc.2015.18.1.73
13. Liang X, Yu J, Wen B, Xie J, Cai Q, Yang Q. MRI and FDG-PET/CT based assessment of axillary lymph node metastasis in early breast cancer: a meta-analysis. Clin Radiol. 2017 Apr;72(4):295-301. doi: 10.1016/j.crad.2016.12.001.
14. Panareo, S., Urso, L., Nieri, A., Caracciolo, M., Valpiani, G., Torricelli, P., Frassoldati, A., Cittanti, C., Rollo, M., & Bartolomei, M. Clinical-Diagnostic Relevance of Breast ―Incidentaloma‖ Detected During 18F-Fluoro-2-Deoxy-D-Glucose Positron Emission Tomography/Computed Tomography: Correlation with Radiological Imaging and Histopathology. Indian Journal of Nuclear Medicine : IJNM : The Official Journal of the Society of Nuclear Medicine, India. 2021; 36. https://doi.org/10.4103/ijnm.ijnm_52_21.
15. Job, S. The Role of Mammography and Ultrasonography in the Evaluation of Breast Masses. journal of medical science and clinical research. 2017; 5. https://doi.org/10.18535/jmscr/v5i9.08.
16. Runjjala, K., & Naidu, Y. Combined Mammographic and Sonomammographic Evaluation of Breast Masses. . 2020; 5. https://doi.org/10.21276/ijcmsr.2020.5.1.36
17. Kanumuri, S., Ramana, K., & Sachar, S. Role of Mammography and Ultrasound in the Evaluation of Palpable Breast Masses with Histopathological Correlation. International Journal of Contemporary Medicine, Surgery and Radiology. 2019 https://doi.org/10.21276/ijcmsr.2019.4.2.4
18. Moschetta, M., Telegrafo, M., Triggiani, V., Rella, L., Cornacchia, I., Serio, G., Ianora, A., & Angelelli, G. Diabetic mastopathy: A diagnostic challenge in breast sonography. Journal of Clinical Ultrasound. 2015; 43. https://doi.org/10.1002/jcu.22246.
19. Sohn, Y., Hong, I., & Han, K. Role of [18F]Fluorodeoxyglucose Positron Emission Tomography—Computed Tomography, Sonography, and Sonographically Guided Fine–Needle Aspiration Biopsy in the Diagnosis of Axillary Lymph Nodes in Patients With Breast Cancer. Journal of Ultrasound in Medicine. 2014; 33. https://doi.org/10.7863/ultra.33.6.1013.
20. Parashar, S., Arora, J., & Mittal, A. Bright Is Not Always Better: A Pictorial Review of Hyperechoic Malignant Breast Masses. The Indian Journal of Radiology & Imaging. 2023; 33. https://doi.org/10.1055/s-0043-1768641.
21. Gopinath, D., Reddy, K., & Murthy, P. Sonographic Characterization of breast masses with pathological correlation. 2020; 3. https://doi.org/10.33545/26644436.2020.v3.i3b.126.
22. Yücesoy, C., Oktay, N., Oztürk, E., Oktay, M., Hücümenoğlu, S., Alper, M., & Hekimoğlu, B. Pathologic assessment of non-palpable probably benign breast masses at sonography: can instant intervention be avoided and is follow-up adequate?. JBR BTR : organe de la Societe royale belge de radiologie (SRBR) = orgaan van de Koninklijke Belgische Vereniging voor Radiologie. 2010; 93 5. https://doi.org/10.5334/jbr-btr.328
23. Fujioka, T., Kubota, K., Toriihara, A., Machida, Y., Okazawa, K., Nakagawa, T., Saida, Y., & Tateishi, U. Tumor characteristics of ductal carcinoma in situ of breast visualized on [F-18] fluorodeoxyglucose-positron emission tomography/computed tomography: Results from a retrospective study.. World journal of radiology. 2016; 8 8. https://doi.org/10.4329/wjr.v8.i8.743.